Guanidine Hydrochloride-Induced Denaturation of the Colicin E1 Channel Peptide: Unfolding of Local Segments Using Genetically Substituted Tryptophan Residues†

Brian A. Steer and A. Rod Merrill*

Guelph−Waterloo Centre for Graduate Work in Chemistry, Department of Chemistry and Biochemistry, University of Guelph, Guelph, Ontario, Canada N1G 2W1

Received January 11, 1995; Revised Manuscript Received March 15, 1995®

ABSTRACT: The soluble colicin E1 channel peptide has a roughly spherical, highly α-helical, compact structure. The structural unfolding properties of the colicin E1 channel peptide were analyzed using fluorescence techniques. The guanidine hydrochloride-induced unfolding pattern of the wild-type channel peptide was examined by monitoring intrinsic tryptophan fluorescence. Additionally, peptide unfolding was examined with the fluorophore, 1-anilinonaphthalene-8-sulfonic acid. In order to probe the unfolding of local segments, single-tryptophan channel peptides were constructed by site-directed mutagenesis. Shifts in fluorescence emission maxima of the single tryptophan residues were used to monitor site-specific unfolding events, in the presence of guanidine hydrochloride. The unfolding patterns reported by tryptophans in different regions of the peptide were diverse. The concentration of guanidine hydrochloride at the unfolding transition midpoint for each mutant peptide and the free energy of unfolding were calculated in order to estimate local segment stabilities. Also, secondary structure unfolding was monitored using circular dichroism spectroscopy. The results of unfolding analysis showed that the channel peptide's unfolding mechanism involves an intermediate structure stabilized by the C-terminal hydrophobic core of the peptide. Knowledge of the unfolding pattern of the soluble channel peptide will aid in the understanding of the secondary and tertiary structural interactions within the channel peptide and the mechanism of colicin E1 activation.

Protein unfolding and refolding patterns can provide useful information about protein structure, stability, and function. Fluorescence spectroscopy is an excellent tool for monitoring denaturant-induced protein unfolding. The fluorescence intensities and emission maxima of intrinsic tyrosine and tryptophan fluorophores are environment sensitive and can thus report unfolding events. Most proteins, however, contain many tyrosine and tryptophan residues, and the contributions of individual fluorophores to overall changes in fluorescence upon unfolding are difficult to ascertain. Therefore, changes in the fluorescence of most proteins upon denaturation estimate only global unfolding events. The use of mutant proteins possessing single tryptophan residues facilitates the probing of site-specific unfolding events using fluorescence spectroscopy (Smith *et al.*, 1991; Royer *et al.*, 1993; Mann *et al.*, 1993).

Here, 11 single-Trp mutants of the colicin E1 channel peptide were used to probe site-specific unfolding events. Colicin E1 is a toxin-like bactericidal protein encoded by a naturally occurring plasmid, ColE1. *Escherichia coli* that harbor the ColE1 plasmid secrete colicin E1. Colicin E1 is lethal to other coliform bacteria that do not possess the colicin plasmid and that bear the vitamin B_{12} receptor. In the cytoplasmic membrane of sensitive cells, colicin E1 forms a lethal ion channel that depolarizes the membrane sufficiently to cause cell death (Gould & Cramer, 1977; Cleveland *et al.*, 1983). Colicin E1 consists of an N-terminal translocation domain, a receptor-binding domain, and a C-terminal channel-forming domain. The channel-forming domain can be isolated conveniently by treatment of whole colicin with protease (Davidson *et al.*, 1984). At acidic pH (≤4) or upon the binding of detergents, the proteolytic channel peptide forms a dissipative ion channel *in vitro* (Bullock *et al.*, 1983; Peterson & Cramer, 1987). The crystal structure of the channel-forming peptide of colicin A (a close relative of colicin E1) has been refined to 2.4 Å resolution (Parker *et al.*, 1989, 1992). The colicin A channel peptide is a globular protein containing 10 α-helical segments and a hydrophobic core consisting of two antiparallel α-helices (helices 8 and 9). Helices 8 and 9 are sequestered from water by eight surrounding amphipathic helices. Various physical studies, including circular dichroism (CD;[1] Brunden *et al.*, 1985), nuclear magnetic resonance (Wormald *et al.*, 1990), and Fourier transform infrared spectroscopy (Rath *et al.*, 1990), have demonstrated that the structural features of the channel peptides of colicins E1 and A are analogous. Parker *et al.* (1989) proposed that helices 8 and 9 form an α-helical hairpin loop that inserts into the membrane bilayer. In colicin E1, it was later determined that helices 8 and 9 form a hydrophobic α-helical hairpin domain buried in the core of the soluble structure (Merrill *et al.*, 1990, 1993), which acts

† This work was supported by the Natural Science and Engineering Research Council of Canada (A.R.M.). B.A.S. was the recipient of a predoctoral scholarship from the Natural Sciences and Engineering Research Council of Canada.

* Author to whom correspondence should be addressed (telephone, 519-824-4120, ext. 3806; fax, 519-766-1499; e-mail, merrill@chembio.uoguelph.ca).

® Abstract published in *Advance ACS Abstracts,* May 1, 1995.

[1] Abbreviations: ANS, 1-anilinonaphthalene-8-sulfonic acid; DMG, dimethylglutaric acid; Gn-HCl, guanidine hydrochloride; Gn-HSCN, guanidine thiocyanate; NATA, *N*-acetyltryptophanamide; CD, circular dichroism; θ, molar ellipticity; C-terminal, carboxy-terminal; $D_{1/2}$, denaturant concentration at unfolding transition midpoint; λ_{em}max, fluorescence emission maximum wavelength.

0006-2960/95/0434-7225$09.00/0

as an anchor in the membrane-bound structure (Song *et al.*, 1991; Shin *et al.*, 1993; Palmer & Merrill, 1994).

In this study, site-specific unfolding events in the colicin E1 channel peptide were investigated using 11 single-tryptophan mutants and fluorescence spectroscopy. In addition, fluorescence changes in the wild-type peptide, as well as the binding of the fluorescent probe, ANS, to the protein, were examined upon unfolding. The unfolding of α-helices, as correlated with decreased molar ellipticities ($\theta_{222\ nm}$), was monitored using CD spectroscopy. The unfolding patterns obtained correlate with existing structural data and the proposed mechanism of activation of the colicin E1 channel peptide.

MATERIALS AND METHODS

Preparation of Mutants and Isolation of Colicin E1 and Its Thermolytic Channel Peptide. Single-Trp mutants of colicin E1 were constructed by site-directed mutagenesis as previously described (Merrill *et al.*, 1993; Steer & Merrill, 1994). Colicin E1 was purified from a lex A^- *E. coli* strain harboring the plasmid $pSKE1^-$ which encoded the appropriate mutant as detailed previously (Merrill *et al.*, 1993; Steer & Merrill, 1994).

Unfolding Conditions. The colicin E1 C-terminal thermolytic channel peptide, in 100 mM NaCl/10 mM dimethylglutaric acid (DMG) buffer (pH 6.0), was mixed with the appropriate amount of 8 M sequanal grade guanidine hydrochloride (Gn-HCl), purchased from Pierce (Rockford, IL), to provide solutions from 0 to 7 M Gn-HCl and 0.1 mg/mL channel peptide, final concentration. For unfolding in guanidine thiocyanate (Gn-HSCN), a 6 M stock solution of the denaturant was prepared by using solid Gn-HSCN purchased from Sigma (St. Louis, MO), and Gn-HSCN/peptide solutions (0−5.5 M) were prepared as described earlier for Gn-HCl. In 1-anilinonaphthalene-8-sulfonic acid (ANS)-binding experiments, 10 μL of 10 mM ANS (Molecular Probes Inc., Eugene, OR) in buffer was added. For circular dichroism spectroscopy, the final peptide concentration was between 0.5 and 1 mg/mL, and the protein was in 100 mM sodium fluoride/10 mM sodium phosphate buffer (pH 7). Peptide concentrations were calculated using the ϵ_M values (280 nm) as reported by Merrill *et al.* (1993). Solutions were incubated at room temperature for a minimum of 30 min prior to spectroscopic analysis because it was determined that this was sufficient time to reach constant values for fluorescence and circular dichroism measurements. Refolding of the channel peptide was examined by diluting wild-type peptide/Gn-HCl solutions with buffer in 0.25 M increments, with a 15 min incubation time (20 °C) between dilutions.

Absorbance Measurements. Absorbance spectra were recorded by using a computer-interfaced Perkin-Elmer Lambda-6 scanning absorbance spectrometer (Perkin-Elmer, Norwalk, CT) with both sample and reference cells at room temperature.

Fluorescence Measurements. Fluorescence spectroscopy was carried out by using a PTI Alphascan-2 spectrofluorometer (Photon Technology Inc., South Brunswick, NJ) with the cell holder thermostated at 20 °C. All spectra were recorded with a 2 nm excitation bandpass and a 4 nm emission bandpass. For all measurements, a wedge depolarizer was placed on the exit side of the excitation monochrometer, and emission was detected at right angles. Wavelength-dependent bias of the optical and detection systems was corrected and appropriate blanks were subtracted. For tryptophan fluorescence, the excitation was 295 nm and the emission was scanned from 303 to 450 nm. The fluorescence emission of ANS was scanned from 390 to 700 nm while the sample was excited at 372 nm.

Temperature Dependence of the Tryptophan Fluorescence of Unfolded Mutant Peptides. The effect of temperature on the tryptophan fluorescence of various mutant unfolded peptides (in 7 M Gn-HCl) was examined. Peptides in 7 M Gn-HCl were cycled through a temperature range from 15 to 80 °C in 5 °C increments. Fluorescence emission spectra were collected at each temperature as described earlier with both the excitation and emission bandpasses at 4 nm.

Circular Dichroism Measurements. CD spectra were recorded at room temperature on a computer-interfaced Jasco J-600 spectrometer using a 0.02 cm path length cuvette. Spectra were obtained with a sensitivity setting of 0.05° full scale and a time constant of 1 s. Each spectrum was an average of five individual spectra and was corrected for any solvent effects by subtracting the appropriate blank. Spectra were recorded from 205 to 250 nm in 0.2 nm increments. Due to the strong absorbance of Gn-HCl, data were not acquired below 205 nm. For CD unfolding profiles, the static ellipticity was measured at 222 nm.

Data Analysis. To obtain unfolding profiles for each mutant peptide, relative shifts in the maxima of tryptophan fluorescence emission spectra were determined and plotted against Gn-HCl concentration. Shifts were quantified by a ratio of the fluorescence at two wavelengths (λ_1 and λ_2). For the unfolding of a given peptide (wild-type or single-Trp mutant), the wavelengths, λ_1 and λ_2, were determined from the emission maxima of the most blue-shifted (0 M Gn-HCl) and the most red- shifted (7 M Gn-HCl) spectra, respectively. The fluorescence (F) at these wavelengths was then used to determine the ratio, $F_{\lambda 1}/F_{\lambda 2}$, for each Gn-HCl concentration, ranging from 0 to 7 M. The ratios were then plotted against the Gn-HCl concentration to generate an unfolding profile. This technique was used to monitor changes in fluorescence upon unfolding because it is insensitive to variations in peptide concentration, thus minimizing experimental error. Unfolding monitored by changes in fluorescence intensity provided qualitatively similar unfolding profiles, but with greater data scatter.

Unfolding transitions were fit by using nonlinear least-squares analysis (MicroCal Origin, MicroCal Software Inc., Northhampton, MA) and the following equation developed by Santoro and Bolin (1988):

$$X_{[D]} = \{(X_N + m_N[D]) + (X_U + m_U[D])\exp[-(\Delta G_{(F\rightarrow U)}/RT + m_G[D]/RT)]\}/\{1 + \exp[-(\Delta G_{(F\rightarrow U)}/RT + m_G[D]/RT)]\}$$

where $X_{[D]}$ is the value of the spectroscopic measurement at a given concentration of denaturant [D], R is the gas constant, and T is the temperature. The remaining six terms are fitting parameters, where X_N and X_U are the values of the spectroscopic measurement extrapolated to zero concentration of denaturant, m_N and m_U are the slopes for the dependencies of X_N and X_U on denaturant concentration, $\Delta G_{(F\rightarrow U)}$ is the free energy between the folded and unfolded states, and m_G

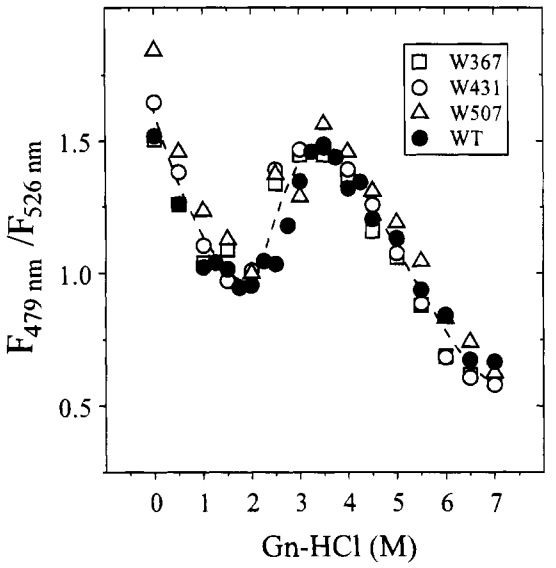

FIGURE 1: Binding of ANS (0.1 mM) to wild-type (●), W367 (□), W431 (○), and W507 (△) channel peptides (0.1 mg/mL) monitored by the fluorescence ratio $F_{479\ nm}/F_{526\ nm}$ as a function of Gn-HCl concentration. The dashed line is drawn through the mean of the data shown. The channel peptide was unfolded as described in Materials and Methods. The fluorescence emission of ANS was scanned from 390 to 700 nm while the sample was excited at 372 nm. The excitation and the emission bandpasses were 2 and 4 nm, respectively.

is the slope describing the dependence of $\Delta G_{(F\rightarrow U)}$ on denaturant concentration. Transition midpoints ($D_{1/2}$ values) were calculated by dividing ΔG by $-m_G$. The transitions of biphasic unfolding profiles were fit independently. Because the second-transition baselines of the biphasic unfolding profiles were not defined, the parameter X_U was fixed to the value of the last point in the transition, with the slope for the dependence of X_U on denaturant concentration set to zero.

RESULTS

Colicin E1 Channel Peptide Mutants. The channel peptide has three naturally occurring Trp residues located at positions 424, 460, and 495. Two of the three Trp residues were replaced by Phe to generate the three single-Trp mutants W424, W460, and W495 (Merrill & Cramer, 1990). Furthermore, all three native Trp residues were replaced with Phe to give a Trp^- mutant, and by replacing either a Phe or a Tyr with a Trp, 11 single-Trp mutants were prepared (Merrill *et al.*, 1993).

Stability of Channel Peptide Mutants. All of the single-Trp mutants have both *in vivo* and *in vitro* channel-forming activity, similar to the wild-type peptide (Merrill & Cramer, 1990; Merrill *et al.*, 1993). Furthermore, the secondary structure of the mutant peptides is analogous to that of the wild-type peptide (ca. 47% α-helix), as determined by CD spectroscopy (Merrill *et al.*, 1993). These data indicate that the mutations do not perturb the structure of the native peptide. Additionally, the mutations do not appear to alter the global unfolding mechanism of the channel peptide. The unfolding profiles of mutant peptides W367, W431, and W507, monitored by ANS binding, were analogous to wild-type unfolding (Figure 1). These three mutant peptides were selected for analysis since none of the tryptophans are naturally occuring and they represent the N-terminal, central, and C-terminal regions of the peptide, respectively. Also, the unfolding profiles of mutant peptides W355 and W495 obtained by CD spectroscopy were comparable to the wild-type peptide unfolding profile (Figure 3). These mutant peptides were chosen for analysis since they represent the least stable (W355) and the most stable (W495) regions of the peptide.

Channel Peptide Unfolding Examined by ANS Binding. Upon unfolding in low Gn-HCl concentrations (0−2 M), ANS binding decreased, as indicated by the concomitant decrease in F_{479}/F_{526} (red shift) with increasing [Gn-HCl] (Figure 1). At 2 M Gn-HCl, however, ANS binding abruptly increased until 4 M Gn-HCl was reached. Subsequent increases in Gn-HCl concentration caused a reduction in the F_{479}/F_{526} value to a minimum of 0.5.

Unfolding and Refolding of Wild-Type Peptide Examined by Tryptophan Fluorescence. The effect of Gn-HCl on tryptophan fluorescence in solution was determined to be negligible by monitoring the fluorescence of *N*-acetyltryptophanamide (NATA) as a function of Gn-HCl concentration (data not shown). This conclusion is corroborated by previous results (Willis & Szabo, 1992). The tryptophan fluorescence emission of the wild-type channel peptide, which contains three tryptophan residues (W424, W460, W495), was monitored by excitation at 295 nm (Figure 2, top left). Upon unfolding, the wild-type tryptophan fluorescence underwent a 26 nm red shift, provided a biphasic unfolding pattern with no significant change in $F_{\lambda 1}/F_{\lambda 2}$ at low Gn-HCl concentrations (below 2 M), and clearly reported the presence of a stable unfolding intermediate that existed in approximately 4 M Gn-HCl. The free energies and transition midpoints for each of the transitions of the biphasic profile were estimated by nonlinear regression (Table 1) as described in Materials and Methods. As a control, the tyrosine fluorescence of a Trp^- channel peptide was monitored upon unfolding (excitation, 280 nm), and no wavelength shift was detectable (data not shown).

Refolding of the channel peptide was examined by diluting wild-type peptide/Gn-HCl solutions with buffer. Upon dilution, in 0.25 M increments, the fluorescence emission of the wild-type peptide underwent a blue shift in its λ_{em}-max analogous to the red shift seen during unfolding (Figure 2).

Analysis of the Unfolding of Local Segments Using Single-Tryptophan Mutants. Eleven single-tryptophan mutants were used to examine site-specific unfolding events within the channel peptide upon titration with Gn-HCl. Each single-Trp mutant peptide had a characteristic tryptophan λ_{em}max when fully folded that can be attributed to the characteristic degree of exposure of each tryptophan in the native peptide to the aqueous medium. The λ_{em}max values of native mutant and wild-type peptides were equivalent to those determined by Merrill *et al.* (1993). However, with the exception of W495, all of the single-Trp peptides had similar tryptophan λ_{em}max values (346−348 nm) when unfolded. The emission maximum of W495 was 334 nm in 7 M Gn-HCl (data not shown).

The unfolding profiles reported for each single tryptophan are shown in Figure 2. For each Gn-HCl concentration, a fluorescence emission spectrum was acquired, and the ratio of fluorescence ($F_{\lambda 1}/F_{\lambda 2}$) was determined as described in Materials and Methods. Tryptophan residues located in the N-terminal half of the channel peptide (W355, W367, W404,

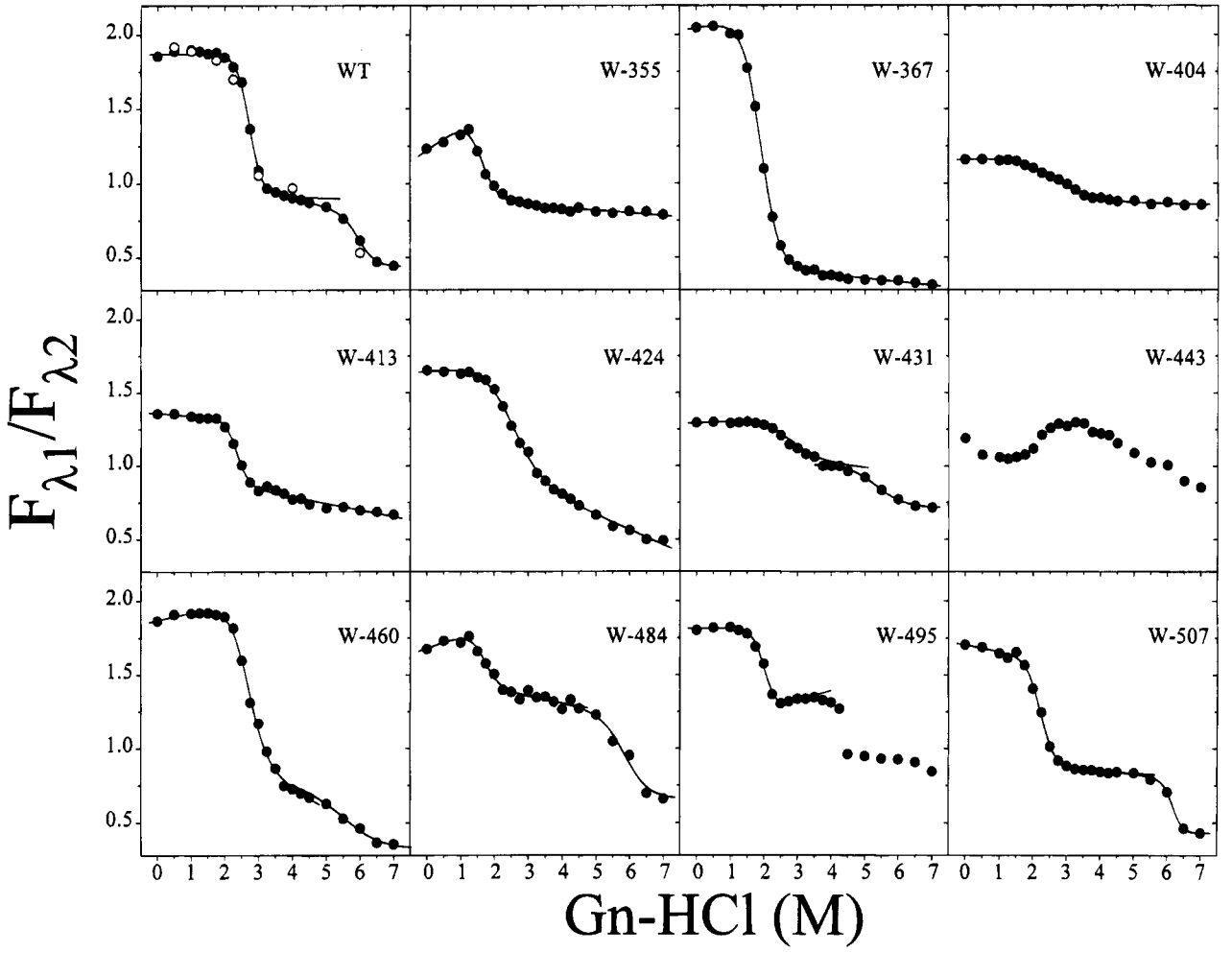

FIGURE 2: Tryptophan fluorescence ($F_{\lambda 1}/F_{\lambda 2}$) for wild-type channel peptide and the 11 mutant single-Trp channel peptides upon unfolding (●) and refolding (○) in Gn-HCl. The lines shown are nonlinear least-squares curves fit to the data. The W443 data and the second transition of W495 were not curve fitted. Peptide concentrations were 0.1 mg/mL, and samples were excited at 295 nm and their emission scanned from 303 to 450 nm. The excitation and emission bandpasses were 2 and 4 nm, respectively. Unfolding conditions were as described in Materials and Methods.

W413, and W424) reported monophasic, but differently shaped, unfolding patterns (Figure 2). The profiles were readily fit by nonlinear regression, and the unfolding free energy ($\Delta G_{(F\rightarrow U)}$) and transition midpoint ($D_{1/2(F\rightarrow U)}$) of each profile were estimated (Table 1). The profile reported by W443 was complicated by an increase in the $F_{\lambda 1}/F_{\lambda 2}$ ratio, and fitting of its unfolding profile was not possible. Tryptophan residues in the C-terminal half of the channel peptide (W431, W460, W484, W495, and W507) reported biphasic unfolding patterns (Figure 2), and like the unfolding profile of wild-type peptide, each transition was fit independently (see Materials and Methods). The free energies associated with each transition ($\Delta G_{(F\rightarrow I)}$ and $\Delta G_{(I\rightarrow U)}$) and the transition midpoints ($D_{1/2(F\rightarrow I)}$ and $D_{1/2(I\rightarrow U)}$) estimated by nonlinear least-squares are shown in Table 1. For the biphasic profiles, the free energy associated with complete unfolding ($\Delta G_{(F\rightarrow U)}$) was estimated by adding the free energies of the individual transitions. Local segments with single Trp residues in the N-terminal two-thirds of the peptide had $\Delta G_{(F\rightarrow U)}$ values between 11 and 32 kJ/mol (Table 1), and residues in the C-terminal segment of the peptide reported much higher $\Delta G_{(F\rightarrow U)}$ values, between 27 and 69 kJ/mol.

Unfolding Monitored by Circular Dichroism Spectroscopy. In order to examine the collapse of channel peptide secondary structure, CD spectra of the wild-type peptide in solutions of 0−7 M Gn-HCl were recorded (data not shown). Due to the strong absorbance of Gn-HCl below 205 nm, CD spectra were only obtained from 205 to 250 nm, thus allowing the evaluation of changes in the α-helical content of the channel peptide only (Figure 3). Unfolding profiles of the change in helical content of the wild-type peptide and the single-Trp mutant peptides, W355 and W495, were generated from CD data ($\theta_{222\ nm}$), and all three peptides produced analogous unfolding profiles (Figure 3). The peptide's secondary structure did not change significantly in relatively low concentrations of denaturant (0−2 M Gn-HCl). Between 2 and 4 M Gn-HCl, α-helical structure began to collapse extensively and reached a minimum at 7 M Gn-HCl. The average of the unfolding profiles was fit by nonlinear least-squares analysis, and the estimated unfolding free energy ($\Delta G_{(F\rightarrow U)}$) was 29 kJ/mol (Table 1).

Unfolding of W495 and W355 Mutant Peptides in Guanidine Thiocyanate. Mutant peptides, W355 and W495, were unfolded in Gn-HSCN by using denaturant solutions from 0 to 5.5 M Gn-HSCN (data not shown). The shapes of the unfolding profiles generated were similar to those shown for Gn-HCl (Figure 2), except that the profiles were shifted along the abscissa to lower denaturant concentrations. The λ_{em}-max of W495 reached 348 nm in 4 M Gn-HSCN and remained at 348 nm in higher denaturant concentrations. The

Table 1: Gibbs Free Energy Values and Unfolding Transition Midpoints Determined from Unfolding Profiles

peptide	$\Delta G_{(F\rightarrow I)}$[a]	$\Delta G_{(I\rightarrow U)}$	$\Delta G_{(F\rightarrow U)}$	$D_{1/2(F\rightarrow I)}$[b]	$D_{1/2(I\rightarrow U)}$	$D_{1/2(F\rightarrow U)}$
CD			29 ± 4			2.6
W355			17 ± 3			1.6
W367			17 ± 1			1.9
W404			11 ± 2			2.6
W413			32 ± 7			2.4
W424			14 ± 2			2.5
W431	17 ± 5	10 ± 2	27 ± 7	2.7	5.4	
W443						
W460	24 ± 4	11 ± 7	35 ± 11	2.6	5.6	
W484	18 ± 8	22 ± 7	40 ± 15	1.7	5.9	
W495	28 ± 6			2.0		
W507	26 ± 3	43 ± 11	69 ± 14	2.2	5.9	
WT	35 ± 6	25 ± 2	60 ± 8	2.8	6.0	

[a] Free energies are in kJ/mol and represent the free energy of unfolding between the folded and the intermediate state (F→I), the intermediate and the unfolded state (I→U), and the folded and the unfolded state (F→U). By using nonlinear least-squares analysis (see Materials and Methods), the free energy of unfolding, $\Delta G_{(F\rightarrow U)}$, which is equal to the free energy of the native state ($-\Delta G_{(F\rightarrow U)} = \Delta G_N$), was calculated from each unfolding profile (Figure 2, fluorescence, and Figure 3, CD). For biphasic transitions, $\Delta G_{(F\rightarrow I)}$ and $\Delta G_{(I\rightarrow U)}$ were determined independently and summed to give $\Delta G_{(F\rightarrow U)}$. The standard errors in ΔG from nonlinear least-squares analysis are shown. The error in $\Delta G_{(F\rightarrow U)}$ for biphasic unfolding profiles is the additive error of $\Delta G_{(F\rightarrow I)}$ and $\Delta G_{(I\rightarrow U)}$. [b] $D_{1/2}$ denotes the midpoints of the F→I, I→U, and F→U transitions in mol/L. $D_{1/2}$ values were calculated by dividing the free energy of the transition by $-m_G$ (the slope describing the dependence of free energy on denaturant concentration).

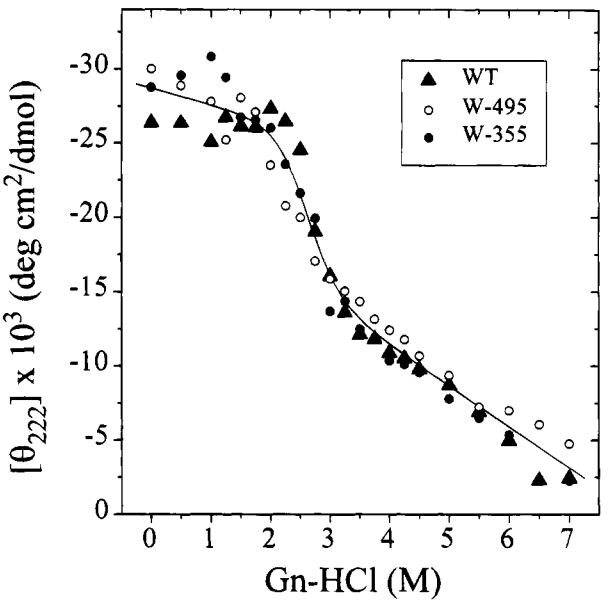

FIGURE 3: Secondary structure unfolding profiles of wild-type (▲), W355(●), and W495 (○) peptides generated, using far-UV circular dichroism, by plotting molar ellipticity (θ) at 222 nm as a function of Gn-HCl concentration, showing the nonlinear least-squares fit through the average of the data. Conditions for CD measurement and analysis were as described in Materials and Methods.

λ_{em}max of W355 reached a constant value (348 nm) in 2 M Gn-HSCN.

Examination of Mutant Peptide Fluorescence in 7 M Guanidine Hydrochloride as a Function of Temperature. The fluorescence as a function of temperature of the single-Trp mutant peptides W367, W404, W484, W495, and W507 in 7 M Gn-HCl was examined. Mutant peptides W367 and W404, which are located in the least stable region of the peptide, in 7 M Gn-HCl, reported no change in Trp λ_{em}max

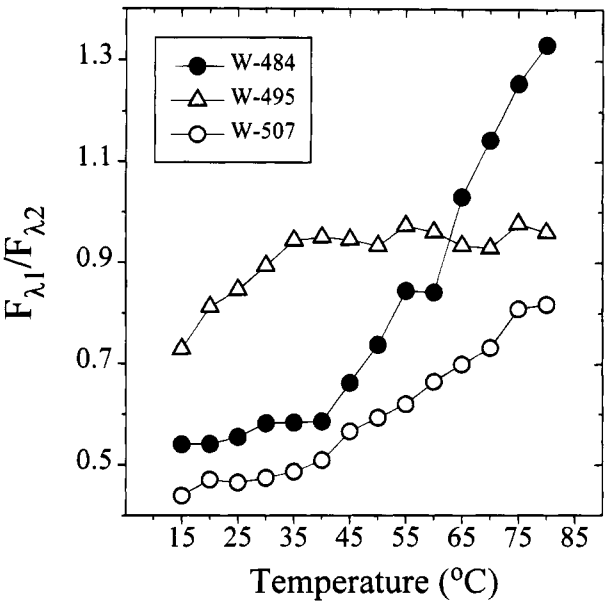

FIGURE 4: Tryptophan fluorescence ($F_{\lambda 1}/F_{\lambda 2}$) of mutant peptides W484 (●), W495 (△), and W507 (○) in 7 M Gn-HCl as a function of temperature. Peptide concentrations were 0.1 mg/mL, and samples were excited at 295 nm and their emission scanned from 303 to 450 nm. The excitation and emission bandpasses were 4 nm. Unfolding conditions were as described in Materials and Methods.

with increasing temperature (data not shown). However, the λ_{em}max values of mutant peptides W484, W495, and W507 in 7 M Gn-HCl, which are located in the most stable region of the peptide and report biphasic unfolding, all underwent blue shifts with increasing temperature (Figure 4).

DISCUSSION

The unfolding of the wild-type channel peptide, as detected by tryptophan fluorescence (Figure 2), provided a biphasic unfolding profile. The major unfolding transition had a midpoint ($D_{1/2(F\rightarrow I)}$) of 2.8 M (Table 1). This unfolding profile implied the presence of a stable intermediate structure, which existed in approximately 4 M Gn-HCl. Unfolding of the intermediate structure required even higher Gn-HCl concentrations, with the midpoint for the intermediate's unfolding transition (as reported by W424, W460, and W495 combined) at 6.0 M. The wild-type unfolding profile also showed that, at least in the peptide segments near W424, W460, and W495, no significant unfolding events occurred at low denaturant concentrations (below 2 M). However, site-specific unfolding analysis using single-Trp mutants demonstrated that, although small, some isolated structural rearrangements occurred at low Gn-HCl concentrations. At low Gn-HCl concentrations, the most obvious small structural changes within the channel peptide involved W355 and W443 (Figure 2).

The binding of ANS to the peptide as a function Gn-HCl concentration also implied that changes in structure occurred at Gn-HCl concentrations below 2 M (Figure 1). The fluorescence emission of ANS undergoes a blue shift and an increase in intensity when the probe is exposed to a hydrophobic environment. It has been shown that ANS binds to nonpolar sites on protein surfaces, with subsequent changes in its fluorescence emission (Stryer, 1965; Bertazzon *et al.*, 1990; Chaffotte *et al.*, 1992). For denaturant concen-

trations up to 2 M Gn-HCl, however, ANS binding actually decreased (Figure 1), suggesting that perhaps nonpolar sites became less exposed. The apparent decrease in ANS binding most likely did not involve significant changes in the peptide's structure, as unfolding examined by both CD (Figure 3) and Trp fluorescence spectroscopic methods (Figure 2) reported no significant structural changes in Gn-HCl concentrations below 2 M. The change in ANS binding most likely involved salt effects. The ionic influence of low Gn-HCl (salt) concentrations may have masked charge−charge interactions at the protein surface and influenced ANS binding. At Gn-HCl concentrations between 2 and 4 M, ANS binding increased (Figure 1). This increase in ANS binding likely resulted from the exposure of the peptide's nonpolar core since it corresponds to the major unfolding transition reported by the wild-type peptide between 2 and 3 M Gn-HCl (Figure 1, top left). Maximum ANS binding occurred at 4 M Gn-HCl, reflecting the intermediate structure reported for the wild-type peptide by Trp fluorescence. As the Gn-HCl concentration was increased, the peptide's structure fully collapsed and ANS binding steadily decreased to a minimum as hydrophobic clustering was eliminated.

Detailed peptide unfolding information was made possible by site-specific unfolding analysis, which exploited the use of single-Trp mutants. Characteristic unfolding patterns were depicted by each of the 11 single tryptophan residues hosted by their respective single-Trp mutant channel peptides (Figure 2). It is important to note that one caveat to this method of site-specific unfolding analysis is that the mutations introduced into the peptide could perturb the peptide's structure, thus altering its unfolding mechanism. However, previous results have demonstrated that these mutations do not cause detectable structural perturbations in the peptide. All of the mutants have normal (wild-type) levels of both *in vivo* and *in vitro* activity, and native mutant peptides have CD spectra analogous to that of the wild type (Merrill *et al.*, 1990, 1993). It should also be noted that all of the mutant proteins' sensitivity to the thermolysin protease was identical to that of the wild-type protein (Merrill *et al.*, 1993).

Adequate determination of the stability of the unfolding equilibria of the mutant peptides by an independent method has proven difficult. However, the unfolding profiles of W355, W495, and wild-type peptides, monitored by CD, were alike (Figure 3). Unfolding of the mutant peptides W355 and W495 specifically was conducted since these residues are located in the least and most stable regions of the peptide, respectively. In addition, the unfolding profiles (ANS binding) of mutant peptides W367, W431, and W507 were analogous to the unfolding profile of the wild-type peptide determined by ANS fluorescence (Figure 1). These three mutant peptides were selected for analysis as none of the tryptophans are naturally occurring. Tryptophan residues that are not native would be the most likely candidates to cause structural perturbations. Furthermore, these tryptophan residues are representative of the N-terminal, central, and C-terminal regions of the peptide. Thus, the conservative amino acid substitutions introduced into the mutants employed in this study do not appear to destabilize the peptide's unfolding equilibria.

Tryptophan residues, W355 and W367 located within the peptide's N-terminal region provided single phase unfolding profiles (Figure 2) with very low $D_{1/2(F\rightarrow U)}$ values (Table 1). Although considered monophasic, the unfolding profile of residue W355 had a small initial phase where W355 underwent an increase in $F_{\lambda 1}/F_{\lambda 2}$ between 0 and 1.25 M Gn-HCl. This increase seen in the unfolding profile at low Gn-HCl concentrations suggests that either the intrinsic quenching of W355 is alleviated or W355 becomes less exposed to solvent. Residue W367 provided a low $D_{1/2(F\rightarrow U)}$ value but underwent a large 28 nm shift in its λ_{em}max, suggesting that its environment in the native peptide is quite hydrophobic. Indeed, by structural alignment with colicin A and helical wheel analysis, the proposed location of W367 is on the hydrophobic face of helix 2.

In order to compare local segment stabilities, Gibbs free energies were estimated (Table 1) by applying the linear extrapolation method originally described by Pace (1986). However, the data were fit by using nonlinear regression and the combined equation developed by Santoro and Bolin (1988). In order to estimate the free energy of unfolding, the unfolding mechanism must be reversible, and as shown (Figure 2) unfolding of the channel peptide was reversible. The accuracy of the free energy values determined by the linear extrapolation method is not considered high, but has been shown to provide reasonable free energy estimates (Cupo & Pace, 1983; Pace, 1986, 1990; Seckler & Jaenicke, 1992). The free energy of unfolding, $\Delta G_{(F\rightarrow U)}$, is also an estimate of the stability of the native state (ΔG_N) as $\Delta G_N = -\Delta G_{(F\rightarrow U)}$, and for most proteins it is between −20 and −60 kJ/mol (Seckler & Jaenicke, 1992; Creighton, 1993).

The free energies of unfolding reported for W355 and W367 indicate that the peptide segment containing these two residues is not highly stable ($\Delta G_N = 17$ kJ/mol). These data are consistent with previous studies that showed that this segment of the peptide undergoes a significant structural change at low pH (≤4; Merrill *et al.*, 1993) or upon the binding of detergent (Steer & Merrill, 1994). Also located in the N-terminal region of the peptide is W404, which exhibits a very broad unfolding profile (Figure 2) due to the small change in its λ_{em}max. This tryptophan does not sense a large unfolding, and compared to the other single tryptophans, its environment is similar in both the native and unfolded peptides, suggesting that it is surface exposed in the folded peptide. This notion is supported by an earlier report that indicated that W404 is located near the surface in the native peptide (Merrill *et al.*, 1993). Indeed, at 11 kJ/mol, the free energy associated with unfolding of the W404 locale is low.

The unfolding pattern reported by W443 is complex, and its complexity is most likely due to an intrinsic quenching process. If this tryptophan were in close proximity to a thiol, a carboxylate, or a histidine residue, then its fluorescence could be quenched. Unfolding would alleviate quenching and provide an unfolding profile much like that reported for W443. One plausible explanation for the observed profile is that, initially upon unfolding, an increase in $F_{\lambda 1}/F_{\lambda 2}$ occurs, but as unfolding progresses further and the tryptophan becomes more exposed, it is quenched by the aqueous solvent, resulting in a decrease in $F_{\lambda 1}/F_{\lambda 2}$. However, since the 3D structure of the colicin E1 channel peptide has not yet been solved, it is impossible to identify the chemical moiety that might be responsible for the intrinsic quenching of W443 fluorescence. Although the unfolding profile reported by W443 is complex, this residue does report significant structural changes at high Gn-HCl concentrations (3−5 M; Figure 2).

The C-terminal region of the colicin E1 channel peptide is distinctly hydrophobic and has been shown in numerous studies to be buried within the core of the peptide (Merrill *et al.*, 1990, 1993; Steer & Merrill, 1994). Interestingly, single Trp residues that report the presence of a stable and partially unfolded intermediate structure, as exhibited by their biphasic unfolding profiles (W431, W460, W484, W495, and W507), are all located within the C-terminal region of the channel peptide. These residues all have high $D_{1/2(I\rightarrow U)}$ values (Table 1) that average 5.7 M. This mean $D_{1/2(I\rightarrow U)}$ value represents the transition midpoint for the intermediate's unfolding. Notably, it is comparable to the $D_{1/2(I\rightarrow U)}$ value for the wild-type peptide, which is likely the result of the second unfolding transition reported for W460 and W495 combined. Clearly, this C-terminal region of the peptide is highly resistant to unfolding by Gn-HCl. It should be noted, however, that although more centrally located within the peptide, W443 reports a second transition at high Gn-HCl concentration, and it may also be involved in the unfolding intermediate.

It should also be noted that the peptide appears to possess some residual structure in 7 M Gn-HCl. All but one of the single Trp residues reported λ_{em}max values between 346 and 348 nm in 7 M Gn-HCl (data not shown). These maxima are comparable to the λ_{em}max values of NATA in solution (350 nm) and thus represent solvent-exposed residues. However, the λ_{em}max for W495 only reached 334 nm in 7 M Gn-HCl, which strongly suggests that W495 was not fully exposed to solvent. This result implies that in 7 M Gn-HCl the peptide segment encompassing W495 might contain some residual structure.

In order to confirm that the blue-shifted λ_{em}max of W495 (7 M Gn-HCl) was the result of residual structure, the W495 peptide was unfolded in the stronger denaturant, Gn-HSCN. As in Gn-HCl, the unfolding profile reported for W495 in Gn-HSCN was biphasic (data not shown). However, in 4 M Gn-HSCN, W495 was fully exposed since its λ_{em}max was 348 nm. At higher Gn-HSCN concentrations (up to 5.5 M), the λ_{em}max of W495 remained unchanged at 348 nm. Clearly, in 7 M Gn-HCl the peptide segment in the region of W495 maintains some residual structure. As a control, W355 was unfolded in Gn-HSCN (data not shown), and it reached an λ_{em}max of 348 nm in 2 M Gn-HSCN and provided a monophasic unfolding profile similar to its profile in Gn-HCl.

In order to examine the nature of the residual structure, the fluorescence of W495 in 7 M Gn-HCl was examined as a function of temperature (all previous fluorescence measurements were taken at 20 °C). Interestingly, W495 underwent a blue shift in its λ_{em}max with increasing temperature, exhibiting a break point near 40 °C (Figure 4). In addition, the fluorescence of residues W484 and W507 (7 M Gn-HCl) also underwent a blue shift with increasing temperature (Figure 4). However, the λ_{em}max values of W355 and W404 (7 M Gn-HCl), which would not be expected to be involved in the residual structure, did not change with temperature (data not shown). Therefore, the enhancement of the hydrophobic effect by increased temperature likely caused residues in the C-terminal hydrophobic region to cluster and become less solvent exposed, especially considering the ionic strength of Gn-HCl. The residual structure reported for W495 in 7 M Gn-HCl (20 °C) could conceivably act as a nucleus for the clustering of other hydrophobic portions of the nonpolar core of the peptide. Several other unfolding studies have found that, for some proteins, residual structures consisting of fluctuating hydrophobic clusters do exist at high denaturant concentrations (Makhatadze & Privalov, 1992; Neri *et al.*, 1992; Pace *et al.*, 1992).

As anticipated, the stability of the C-terminal peptide region, which is involved in the residual structure, is quite high (ΔG_N values for peptide segments containing W460, W484, and W507 are −35, −40, and −69 kJ/mol, respectively). The ΔG_N for the peptide segment containing W495 could not be determined since W495 did not fully unfold in Gn-HCl. However, the free energy associated with the unfolding transition to the intermediate, $\Delta G_{(F\rightarrow I)}$, for the W495 segment was 28 kJ/mol. Additional free energy would be required to unfold the intermediate, and thus a significant amount of energy would be required to fully unfold the W495 locale.

The intermediate state free energies for the other regions of the peptide associated with the intermediate structure, containing W460, W484, and W507, were also determined (Table 1). Generally, these free energy values are similar to the values for complete unfolding of the N-terminal portion of the peptide. It may be that the first unfolding transition reported by these residues partially represents the unfolding of the N-terminal region, as the buried residues may become more exposed as the N-terminal segment unfolds.

It is of interest that residues W484, W495, and W507 are all contained within a functionally significant hydrophobic stretch of the peptide spanning from A474 to I508. This region is believed to be responsible for initially penetrating the membrane bilayer, where it then forms the hydrophobic α-helical hairpin in the membrane-bound channel peptide (Figure 5) as previously described (Song *et al.*, 1991; Zhang & Cramer, 1992; Shin *et al.*, 1993; Palmer & Merrill, 1994).

The intermediate partially unfolded peptide structure appears to contain little significant secondary structure, although the estimation of secondary structure in high denaturant concentration is not very reliable (R. Woody, personal communication). Unfolding examined by CD ($\theta_{222\ nm}$) was monophasic (Figure 3) with a $D_{1/2(F\rightarrow U)}$ value of 2.6 M. The profile did not clearly indicate the presence of a stable intermediate structure. Because the dichroism signal is a composite value originating from all of the peptide bonds in the protein, CD spectroscopy would be expected to be less sensitive for detecting the intermediate structure sensed by site-specific unfolding analysis using tryptophan fluorescence, especially considering that the intermediate structure likely has little or no secondary structure. Thus, the ΔG_N value determined from the CD unfolding profile, −29 kJ/mol, was much lower than the values reported for peptide segments involved in the intermediate (Table 1). Furthermore, the highly stable C-terminal region only encompasses a small portion of the peptide and most likely does not markedly affect the global stability (represented by the ΔG_N value from CD) of the protein.

The ΔG_N determined for the unfolding of wild-type peptide (−60 kJ/mol), as monitored by Trp fluorescence, was much higher than the ΔG_N obtained from CD (−29 kJ/mol). The tryptophan fluorescence of the wild-type peptide involves three residues (W424, W460, and W495), two of which are involved in the intermediate unfolded structure (W460 and W495) and give rise to the higher ΔG_N value. Also, the unfolding reported by these Trp residues may be complicated

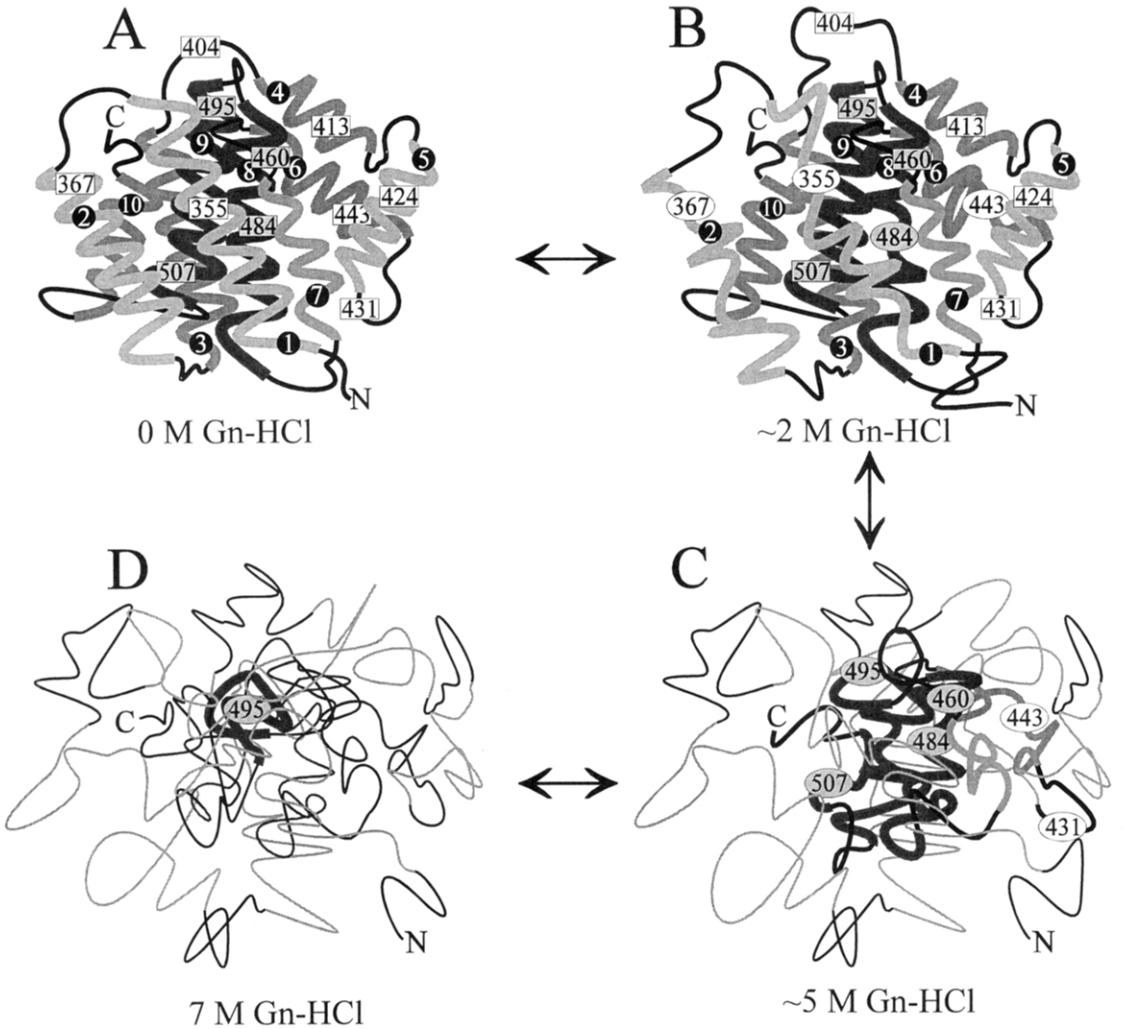

FIGURE 5: Model illustrating the unfolding of the colicin E1 channel peptide. Only the general topological positions of the helices and labeled residues are implied. (A) Native state (0 M Gn-HCl). The hydrophobic α-helical hairpin is shown in dark gray and the helices are numbered with black circles. Tryptophan positions are numbered within a rectangle, and shaded rectangles represent tryptophans that are involved in the intermediate. (B) Small structural rearrangements that occur in about 2 M Gn-HCl. Tryptophans that are involved in structural rearrangements are outlined with an ellipse. (C) The partially unfolded intermediate (~5 M Gn-HCl). Tryptophans located in regions that retain structure (bold lines) are outlined with an ellipse. Regions that are fully unfolded are shown as thin lines, and tryptophans located within these peptide segments are not labeled. (D) Unfolded peptide (7 M Gn-HCl) with a residual hydrophobic cluster (bold lines) involving Trp-495.

by fluorescence resonance energy transfer processes (manuscript in preparation). These results demonstrate that the method used to monitor unfolding can markedly affect free energy estimations. A protein's global free energy of unfolding, estimated from the fluorescence signal of only a few intrinsic residues, may not always be valid.

A model has been proposed to illustrate the pattern of unfolding envisioned for the colicin E1 channel peptide (Figure 5). The native peptide structure (0−2 M Gn-HCl) remains intact, although some slight structural rearrangements may occur. In 2−5 M Gn-HCl, the peptide undergoes significant loss of α-helical content and a large unfolding transition as reported by most single Trp residues. However, in approximately 5 M Gn-HCl, an intermediate partially folded structure (low in secondary structure content) persists that primarily involves the C-terminal hydrophobic region of the peptide, containing residues W460, W484, W495, and W507. Further denaturation results in the disintegration of the hydrophobic folding core, resulting in mostly a random coil structure but appears to retain a small amount of hydrophobic residual structure near W495.

The active insertion-competent state of the peptide, induced by the binding of detergent or by a low-pH medium (≤4), involves a subtle unfolding of tertiary structure with mostly little or no change in secondary structure (Merrill *et al.*, 1993; Steer and Merrill, 1994). The C-terminal hydrophobic core of the peptide becomes more exposed upon activation but remains structurally unaltered. As demonstrated by the present study, this region is stable and resists denaturation, which corroborates the hypothesis that the hydrophobic α-helical hairpin inserts into the membrane bilayer as a unit composed of two tightly bound antiparallel helices connected by a hairpin turn.

This study has demonstrated that single tryptophan residues are valuable tools for reporting the site-specific unfolding events in proteins. A relatively detailed analysis of a protein's folding pathway can be obtained by genetically engineering tryptophan residues into a protein, provided that the mutations do not alter the stability of the protein's unfolding equilibria. When combined with other techniques that monitor folding, tryptophan fluorescence can describe intermediate unfolded states and can give a relatively clear

picture of a protein's folding/unfolding pattern. To further elucidate the unfolding mechanism of the colicin E1 channel peptide, future studies will involve monitoring unfolding by time-resolved fluorescence analysis and the use of other denaturants such as urea. This expanded approach may serve to provide further information on the relative contributions of the electrostatic forces and hydrophobic contacts (hydrophobic effect) to the structural stability of the colicin E1 channel peptide and, furthermore, toward a better understanding of the mechanism of activation of this toxin-like protein.

ACKNOWLEDGMENT

We thank Dr. William Cramer for supplying the *E. coli* strain IT3661 and the colicin E1 plasmid pSKE1$^-$. Furthermore, we thank Dr. Arthur Szabo for critically reviewing the manuscript, and we also thank Dr. Rick Yada and Massimo Marconi for assistance with circular dichroism spectroscopy.

REFERENCES

Bertazzon, A., Tian, G. H., Lamblin, A., & Tsong, T. Y. (1990) *Biochemistry 29*, 291−298.
Brunden, K. R., Uratani, Y., & Cramer, W. A. (1984) *J. Biol. Chem. 259*, 7682−7687.
Bullock, J. O., Cohen, F. S., Dankert, J. R., & Cramer, W. A. (1983) *J. Biol. Chem. 258*, 9908−9912.
Chaffotte, A. F., Cadieux, C., Guillou, Y., & Goldberg, M. E. (1992) *Biochemistry 31*, 4303−4308.
Cleveland, M. B., Slatin, S., Finkelstein, A., & Levinthal, C. (1983) *Proc. Natl. Acad. Sci. U.S.A. 80*, 8706−8710.
Creighton, T. E. (1993) *Proteins: Structure and Molecular Properties*, p 291, W. H. Freeman and Company, New York.
Cupo, J. F., & Pace, C. N. (1983) *Biochemistry 22*, 2654.
Davidson, V. L., Brunden, K. R., & Cramer, W. A. (1985) *Proc. Natl. Acad. Sci. U.S.A. 82*, 1386−1390.
Gould, J. M., & Cramer, W. A. (1977) *J. Biol. Chem. 252*, 5491−5497.
Makhatadze, G. I., & Privalov, P. L. (1992) *J. Mol. Biol. 226*, 491−505.
Mann, C. J., Royer, C. A., & Matthews, C. R. (1993) *Protein Sci. 2*, 1853−1861.
Merrill, A. R., & Cramer, W. A. (1990) *Biochemistry 29*, 8529−8534.
Merrill, A. R., Cohen, F. S., & Cramer, W. A. (1990) *Biochemistry 29*, 5829−5836.
Merrill, A. R., Palmer, L. R., & Szabo, A. G. (1993) *Biochemistry 32*, 6974−6981.
Neri, D., Billeter, M., Wider, G., & Wüthrich, K. (1992) *Science 257*, 1559−1563.
Pace, C. N. (1986) *Methods Enzymol. 131*, 266−280.
Pace, C. N. (1990) *Trends Biochem. Sci. 15*, 14−17.
Pace, C. N., Laurents, D. V., & Erickson, R. E. (1992) *Biochemistry 21*, 2728−2734.
Palmer, L. R., & Merrill, A. R. (1994) *J. Biol. Chem. 269*, 4187−4193.
Parker, M. W., Pattus, F., Tucker, A. D., & Tsernoglou, D. (1989) *Nature 337*, 93−96.
Parker, M. W., Postma, J. P. M., Pattus, F., Tucker, A. D., & Tsernoglou, D. (1992) *J. Mol. Biol. 224*, 639−657.
Peterson, A. A., & Cramer, W. A. (1987) *J. Membr. Biol. 99*, 197−204.
Rath, P., Bousche, O., Merrill, A. R., Cramer, W. A., & Rothchild, K. J. (1991) *Biophys. J. 59*, 516−522.
Royer, C. A., Mann, C. J., & Matthews, C. R. (1993) *Protein Sci. 2*, 1844−1852.
Santoro, M. M., & Bolin, D. W. (1988) *Biochemistry 27*, 8063−8068.
Seckler, R., & Jaenicke, R. (1992) *FASEB J. 6*, 2545−2552.
Shin, Y.-K., Levinthal, C., Levinthal, F., & Hubbel, W. L. (1993) *Science 259*, 960−963.
Song, H. Y., Cohen, F. S., & Cramer, W. A. (1991) *J. Bacteriol. 173*, 2927−2934.
Steer, B. A., & Merrill, A. R. (1994) *Biochemistry 33*, 1108−1115.
Stryer, L. (1965) *J. Mol. Biol. 13*, 482−495.
Willis, K. J., & Szabo, A. G. (1992) *Biochemistry 31*, 8924−8931.
Wormald, M., Merrill, A. R., Cramer, W. A., & Williams, R. J. P. (1990) *Eur. J. Biochem. 191*, 155−165.
Zhang, Y.-L., & Cramer, W. A. (1992) *Protein Sci. 1*, 1666−1676.

BI950061N